Control-Informed Wave Prediction for Wave Energy Conversion

Siyuan Zhan, *Member, IEEE*, and John V. Ringwood, *Life Fellow, IEEE*

***Abstract*—Energy maximization (EM) control for wave energy converters (WECs) is a noncausal control approach that explicitly or implicitly involves feedforward from future wave predictions. In the current noncausal control paradigm, the wave prediction problem and the control problem are considered separately. However, there is a lack of theoretical studies that elucidate the mechanism by which inaccuracies in wave prediction deteriorate EM control performance. This brief aims to address this gap by integrating control considerations into the development of wave predictors. Based on the assumption of a linear WEC, the brief first revisits the linear noncausal optimal control (LNOC) problem, establishing the connections between the control and wave prediction problems. Assuming a known wave spectrum, it is shown that the linear Gaussian process (GP)-based excitation force predictor, which optimizes the conditional covariance of excitation force prediction, also maintains statistical optimality in the WEC EM control problem. Subsequently, a novel time-series-based approach for direct acausal estimation is presented, which achieves the same performance as the optimal predictor but with significantly fewer parameters to determine. The implementation in practical scenarios with an unknown wave spectrum is also discussed. Finally, a numerical simulation, based on a benchmarked point absorber WEC (PA-WEC), is presented to demonstrate the implementation process and the efficacy of the developed predictor.**

***Index Terms*—Optimal control, wave energy, wave prediction.**

I. Introduction

WAVE energy has the potential to contribute to carbon-zero goals for countries and regions, with 29 500 TW exploitable wave resources worldwide [1], but current technology is economically uncompetitive compared to wind and solar. Studies [2] and [3] reviewed that effective energy maximization (EM) control strategies can significantly improve the energy capture of WECs, without a notable increase in installation and operation cost, which reduces the unit cost of wave energy.

The EM control problem for WECs is essentially a noncausal optimal control problem; that is, by using information on future waves, the energy conversion efficiency can be significantly increased [4]. Based on this principle, many noncausal optimal control algorithms have been developed for WECs, which can incorporate the recursively updated wave prediction to increase conversion efficiency, including those methods based on dynamic programming [5], approximate dynamic programming [6], and model-predictive control [7], [8], [9].

When a WEC can be described by a representative linear model, previous studies [10], [11] show that, at the cost of not explicitly handling hard constraints, the noncausal WEC EM control problem can be solved with a closed-form linear noncausal optimal control (LNOC) law, consisting of a causal feedback part of the WEC states, and an acausal feedforward part of wave excitation force (WEF) estimation. The design process of LNOC can be completed offline, and the implementation does not require online computation, which makes it particularly attractive for WECs with complex linear dynamics, for example, M4 in small to medium oscillations [12].

As most wave elevation and WEF predictors share similar techniques, the term "wave prediction" will be used to represent both WEF and elevation cases. Many wave prediction techniques have been proposed and adopted to provide the noncausal information required in WEC EM optimal control, which can be divided into two main categories. The first category predicts future wave elevation, or WEF, using measurements taken at one or more points at a set of up-wave locations. By exploring the dispersion relation, and with an appropriate design of measurement locations, this type of method, for example, deterministic sea wave prediction (DSWP), leads to a deterministic forecast of incoming wave, which can obtain accurate wave prediction for tens of seconds. The second category models the propagation of the wave using time series models, from only the past wave information available at the WEC position. Time-series-based approaches have significant application advantages in terms of hardware requirements, mainly because they only use measurements from the WEC itself [13]. For example, an autoregressive (AR)-based wave height estimator was designed to provide references for the optimal tuning of a resistive controller in a fuzzy logic framework [14]. An AR-based wave elevation predictor was developed in [15] to calculate the optimal velocity reference that leads to the maximized energy output. Recently, an AR-based predictor was developed in [16] to generate future WEF prediction to provide noncausal information for the LNOC.

For most of the operational (i.e., power producing) sea states of WECs, ocean waves satisfy the Gaussian linear process assumption [13], [17], which, for short horizons closer to 20 min, can be further assumed stationary. Based on this property, many time-series-based approaches have been developed to provide essential noncausal information for WEC control. For example, Fusco and Ringwood [18] compares various time series models for surface elevation forecasting, including harmonic models, and linear and artificial neural

Received 27 September 2025; revised 8 December 2025; accepted 20 December 2025. Date of publication 6 February 2026; date of current version 5 May 2026. The work of John V. Ringwood was supported by Taighde Éireann–Research Ireland through the MaREI Centre for Energy, Climate and Marine under Grant 12/RC/2302_P2. Recommended by Associate Editor A. Mesbah. *(Corresponding author: Siyuan Zhan.)*

Siyuan Zhan is with the School of Engineering, Trinity College Dublin, Dublin, D02 PN40 Ireland (e-mail: zhans@tcd.ie).

John V. Ringwood is with the Centre for Ocean Energy Research, Maynooth University, Maynooth, W23 V5XH Ireland (e-mail: john.ringwood@mu.ie).

Digital Object Identifier 10.1109/TCST.2026.3655752

network-based AR models. The results show that a simple linear AR model has good accuracy in swell waves, that is, the sea states with the most energy generation potential. GP-based models are developed in [19] to forecast wave elevation, based on wave spectral and past wave data, which shows prediction optimality, in terms of the conditional covariance of the prediction, assuming the linear stationary Gaussian wave assumption is valid. Despite the major success in applications mentioned above, there is a lack of theoretical foundations that establish the relations between two critical problems, namely, control and wave prediction.

This brief bridges the gap by theoretically investigating the LNOC problem and wave forecasting from an integrated perspective. First, the fundamental control formulation of LNOC (as studied in [10]) is extended to include imperfect predictions. This results in the formulation of a control law that coincides with the perfect prediction case, with the addition of a term articulating the performance degradation induced by wave prediction inaccuracy. In this way, the control law is formulated and the potential performance degradation is quantified before controller implementation. Second, based on this result, and assuming stationary Gaussian waves, it is proved that the GP-based wave predictor leads to optimal control performance. Subsequently, building on this theoretical study, a novel time-series-based direct estimator (DE) is developed to estimate the acausal feedforward component of the LNOC, which preserves optimality, but with significantly fewer model parameters to determine. This feature is particularly useful for implementation in changing sea states or unknown wave spectrum scenarios, as significantly less data are required to initiate or update the DE. Finally, this theoretical study enables the design of a causal control framework to solve the noncausal WEC control problem.

The remainder of the brief is organized as follows. Section II provides preliminaries of the WEC control and prediction problem, including WEC modeling, control problem formulation, the estimation of state, and WEF. Section III formulates the LNOC, where the connection between the control and prediction problems is established. In Section IV, after studying the estimation/prediction problem for the acausal part, a novel DE is developed and some implementation issues are also discussed. Numerical simulation results are presented in Section V. Finally, Section VI concludes the brief.

Notation: Let $\mathbb{R}^n$, and $\mathbb{R}^{a\times b}$, denote the space of all real n-dimensional vectors, and all a-by-b-dimensional matrices, respectively; $0_{n\times m}$ denotes an n-by-m matrix in which all elements are equal to zero; $\mathbb{Z}_{a:b}$ and $\mathbb{Z}_{\geq a}$ denote a set of integers from a to b, and greater than or equal to a, respectively. For column vectors z_1 and z_2, $[z_1, z_2]$ denotes a column vector $[z_1^\top\ z_2^\top]^\top$. $z_{a:b} := [z_a, z_{a+1}, \ldots, z_b]$. For vector $a \in \mathbb{R}^n$, $\|a\|_M := (a^\top M a)^{1/2}$; Σ_{aa} denotes its variance matrix. For two vectors $a \in \mathbb{R}^n$ and $b \in \mathbb{R}^m$, Σ_{ab} denotes the covariance matrix between a and b.

II. Preliminaries

A. Modeling

For demonstration purposes, this brief presents the results based on a PA-WEC restricted to heave motion only, with a focus on predicting the WEF. However, the proposed method is generic and can be applied to other types of WECs with linear models and to predict wave elevation or WEF. Fig. 1 shows the schematic of the PA-WEC. Assuming linear potential flow

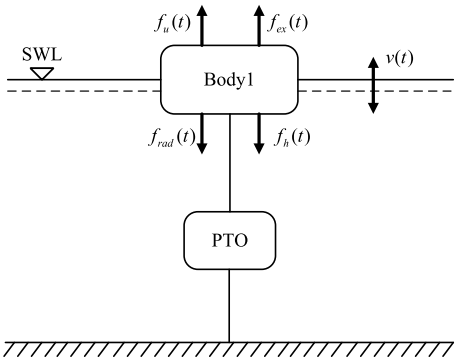

Fig. 1. Dynamic diagram of the float (SWL: still wave level; PTO: power take-off unit; $f_{\text{rad}}(t)$: radiation force; $f_{\text{ex}}(t)$: excitation force; $f_h(t)$: hydrostatic restoring force; $f_u(t)$: PTO/control force; and $v(t)$: heave velocity).

$$m\dot{v}(t) = -f_h(t) - f_{\text{rad}}(t) + f_{\text{ex}}(t) + f_u(t) \tag{1}$$

where m is the mass of the float. $f_u(t)$ is the manipulatable power take-off (PTO) force. $f_{\text{ex}}(t)$ is the WEF. The hydrostatic restoring force $f_h(t)$ is modeled by

$$f_h(t) = k_h z(t) \tag{2}$$

with heave displacement $z(t)$ and hydrostatic stiffness $k_h = \rho g S_w$, where ρ, g, and S_w denote the water density, gravitational acceleration, and the cross-sectional area of the buoy, respectively.

$f_{\text{rad}}(t)$ is the radiation force that models the frequency-dependent damping effect of the heaving oscillated body producing radiated waves to the surrounding fluid. With a standard assumption associated with linear potential theory [20], the radiation force can be modeled by a linear convolution of the radiation impulse response $h_r(t)$ and heave velocity $v(t)$

$$f_{\text{rad}}(t) = \int_{-\infty}^{t} h_r(\tau)\, v(t-\tau)\ d\tau + m_\infty \dot{v}(t) \tag{3}$$

where m_∞ is the added mass asymptote at an infinite frequency. These two terms can be calculated via hydrodynamic codes such as NEMOH [20]. To develop a control-oriented model, a state-space model with minimal realization is used to approximate $f_{\text{rad}}(t)$ in (3)

$$\begin{aligned} \dot{x}_r(t) &= A_r x_r(t) + B_r v(t) \\ f_{\text{rad}}(t) &= C_r x_r(t) + D_r v(t) \approx \int_{-\infty}^{t} h_r(\tau)\, v(t-\tau)\ d\tau \end{aligned} \tag{4}$$

where (A_r, B_r, C_r, D_r) and $x_r \in \mathbb{R}^{n_r}$ are the state-space matrices and the associated state vector, respectively.

With (2) and (3), dynamic equation (1) results in the well-known Cummins' equation [21]

$$\begin{aligned} (m + m_\infty)\dot{v} = f_{\text{ex}}(t) - k_h z(t) \\ - \int_{-\infty}^{t} h_r(\tau)\, v(t-\tau)\ d\tau + f_u(t). \end{aligned} \tag{5}$$

B. WEC Control Problem Setup

Defining the state vector $x(t) := [z(t), v(t), x_r(t)] \in \mathbb{R}^{n_x}$, with the dimension of the state $n_x = 2 + n_r$, the control input $u(t) = f_u(t) \in \mathbb{R}$ and disturbance input $w(t) := f_{\text{ex}}(t) \in \mathbb{R}$, the following state-space model from Cummins' equation (5) can be established:

$$\dot{x}(t) = A_c x(t) + B_{uc} u(t) + B_{wc} w(t) \tag{6}$$

with coefficients

$$A_c = \begin{bmatrix} 0 & 1 & 0_{1\times n_r} \\ -\frac{k_h}{M} & -\frac{D_r}{M} & -\frac{C_r}{M} \\ 0_{n_r\times 1} & B_r & A_r \end{bmatrix}, \quad B_{wc} = B_{uc} = \begin{bmatrix} 0 \\ \frac{1}{M} \\ 0_{n_r\times 1} \end{bmatrix} \tag{7}$$

and $M := m+m_\infty$. The instantaneous power, with consideration of the quadratic dissipation effect in the PTO [22], can be expressed by

$$p(t) := -v(t)\,u(t) - (1/2)\,r u^2(t) \tag{8}$$

with $r > 0$.

Remark 1 (Passivity/Dissipativity): A WEC device is passive, that is, a WEC cannot convert more energy than it absorbs from ocean waves. Due to this passive nature and dissipative effect in the PTO and in the WEC hydrodynamics, a (strict) passivity condition in the energy sense, or equivalently a (strict) dissipativity condition in the signal-theoretical sense, with respect to a supply rate defined as $-p(t)$, needs to be imposed during the WEC modeling process. For passivity-enforcing modeling, or ad hoc passivity restoring methods, please refer to [23] and [24] for details.

To simplify the formulation and to match the receding-horizon implementation manner of LNOC with recursively updated wave prediction, this brief adopts a discrete-time (DT) control formulation similar to [10]. Accordingly, the continuous-time control-oriented model (6) is converted into the following DT model, using the standard zero-order holder (ZOH) convention, with a sampling time period t_s:

$$x_{k+1} = Ax_k + B_u u_k + B_w w_k \tag{9}$$

where (A, B_u, B_w) are the DT state-space matrices.

Following the passivity/dissipativity-preserving discretization approach of [25], the energy captured for one sampling interval starting at k, is modeled by:

$$\begin{aligned} e_k &= \int_{kt_s}^{(k+1)t_s} p(\tau)\; d\tau \\ &= -\left[\frac{1}{2} R u_k^2 + u_k^\top (S_x x_k + S_w w_k)\right] \end{aligned} \tag{10}$$

where $R := t_s r$, $S_x := C_z(A - I)$, $S_w := C_z B_w$, and $C_z := [1 \;\; 0_{1\times(n_x-1)}]$.

Since WEC operation does not have a natural termination, but one can only obtain wave forecasting (with sufficient accuracy) up to a horizon N, WEC EM control aims to solve the following problem at each time instant, recursively, such that the recursive updates on wave excitation prediction can be incorporated:

$$\begin{aligned} \mathcal{P}^N: \; \inf_{\boldsymbol{u}} \; & \sum_{k=0}^{\infty} L(x_k, u_k, w_k) \\ \text{s.t.} \;\; & x_{k+1} = Ax_k + B_u u_k + B_w w_k, \quad k \in \mathbb{Z}_{0:N-1} \\ & x_{k+1} = Ax_k + B_u u_k \quad k \in \mathbb{Z}_{N:\infty} \end{aligned} \tag{11}$$

with stage cost defined as $L(x_k, u_k, w_k) := -e_k = 1/2 R u_k^2 + u_k(S_x x_k + S_w w_k)$, such that minimizing the cost corresponds to maximizing the extracted energy. Following a similar manner to receding horizon control, only the first element of the solution solving $\mathcal{P}_N$, that is, u_0^*, is applied as the control input.

The assumption $w_k = 0$ for $k \geq N$ is motivated by performance considerations. Recent work [26] has shown that this formulation leads to an optimal control law consistent with those obtained from stochastic MPC, where w_k beyond the prediction horizon is modeled as a zero-mean Gaussian distribution. From a physical perspective, setting $w_k = 0$ for $k > N$ can also be interpreted as representing the remaining kinetic energy temporally in the WEC mover, which will eventually be converted into electricity.

III. LNOC Formulation With Imperfect Prediction

This section establishes the connection between the EMC problem $\mathcal{P}^N$, and the prediction problem for WEF.

By partitioning the infinite state trajectory into $\boldsymbol{x}_{0:\infty} = [\boldsymbol{x}_{0:N-1}, \boldsymbol{x}_{N:\infty}]$ and the input trajectory into $\boldsymbol{u}_{0:\infty} = [\boldsymbol{u}_{0:N-1}, \boldsymbol{u}_{N:\infty}]$, the optimal control problem beyond horizon N reduces to a standard unconstrained, undiscounted, and indefinite linear quadratic optimal control (iLQOC) problem, which can be solved analytically in closed form by exploiting the passivity/dissipativity-preserving discretization together with recent results on iLQOC in [27] and [28].

Therefore, the infinite-horizon problem $\mathcal{P}^N$, defined in (11), can be equivalently reformulated as the following finite-horizon control problem:

$$\mathcal{P}^N: \;\; \min_{\boldsymbol{u}} V_0^N, \;\; \text{s.t.} \;\; x_{k+1} = Ax_k + B_u u_k + B_w w_k \tag{12}$$

with the control cost function V_0^N defined as

$$V_0^N := \Sigma_{k=0}^{N-1} L(x_k, u_k, w_k) + (1/2)\, x_N^\top P x_N \tag{13}$$

where the superscript N and subscript 0 represent the prediction length and current time instant, respectively; the stage cost $L(x_k, u_k, w_k)$ is defined in (12), while P is calculated from the following DT algebraic Riccati equation (DARE):

$$P = A^\top PA - \left(S_x + B_u^\top PA\right)^\top \left(R + B^\top PB\right)^{-1} \left(S_x + B_u^\top PA\right). \tag{14}$$

Next, the following results on LNOC, when fully accurate WEF prediction is assumed, are recalled.

Lemma 1: With known $\boldsymbol{w}_{0:N-1}$, $\mathcal{P}^N$ can be solved with

$$u_k^* = K_x x_k + K_w w_k + K_s s_{k+1}, \quad k \in \mathbb{Z}_{0:N-1} \tag{15}$$

where $K_x = -(R + B_u^\top PB_u)^{-1}(S_x + B_u^\top PA)$, $K_w = -(R + B_u^\top PB_u)^{-1}(S_w + B_u^\top PB_w)$, $K_s = -(R + B_u^\top PB_u)^{-1} B_u^\top$, and the time-variant s_{k+1} is determined recursively from the difference equation

$$s_k = \Phi s_{k+1} + \Psi w_k, \quad s_N = 0_{n_x\times 1} \tag{16}$$

with coefficients $\Phi := (A + B_u K_x)^\top$ and $\Psi := \Phi P B_w + K_x^\top S_w$.

Lemma 2: The resultant optimal cost function V_0^{N*} takes a quadratic form in x_0, that is, $V_0^{N*} = 1/2 x_0^\top P x_0 + x_0^\top s_0 + a_0$,

where P and s_0 are determined from (14) to (16), and a_0 depends on $\boldsymbol{w}_{0:N-1}$.

Proof: The proof of Lemmas 1 and 2 is detailed in the proof of Theorem 1 in [29]. □

Based on Lemmas 1 and 2, a LNOC can be developed. The calculation of s from the backward iteration in (16) can be further simplified as

$$\begin{aligned} s_{N-1} &= \Phi s_N + \Psi w_{N-1} = \Psi w_{N-1} \\ s_{N-2} &= \Phi s_{N-1} + \Psi w_{N-2} = \textstyle\sum_{j=N-2}^{N-1} \Phi^{j-N+2} \Psi w_j \\ &\vdots \\ s_1 &= \Phi s_2 + \Psi w_{N-2} = \textstyle\sum_{j=1}^{N-1} \Phi^{j-1} \Psi w_j. \end{aligned}$$

Remark 2: The corresponding optimal control policy, with accurate prediction information on WEF, can be further simplified into matrix multiplication

$$\begin{aligned} u_0^* &= K_x x_0 + K_w w_0 + K_s s_1 \\ &= K_x x_0 + K_d \boldsymbol{w}_{0:N-1} \end{aligned} \tag{17}$$

where $K_d := \begin{bmatrix} K_w & K_s\Psi & K_s\Phi\Psi & \dots & K_s\Phi^{N-2}\Psi \end{bmatrix}$.

So far, the LNOC (17) is formulated in a matrix multiplication form, which consists of 1) a feedback part (causal) from the current state $u_{fb,0} := K_x x_0$ and 2) a feedforward part (noncausal) from the predicted disturbance sequence $u_{ff,0} := K_d \boldsymbol{w}_{0:N-1}$.

However, in reality, perfect information on the future excitation force cannot be retrieved, and the use of imperfect previews will inevitably result in performance degradation. To establish the connection between prediction error for WEF and the control performance for LNOC, the formulation of the joint control and prediction problem is initially tackled by denoting the imperfectly predicted wave prediction sequence by

$$\hat{\boldsymbol{w}}_{0:N-1} := [\hat{w}_0, \hat{w}_1, \dots, \hat{w}_{N-1}] \tag{18}$$

and the controller using imperfect wave preview as

$$\hat{u}_0^* := K_x x_0 + K_d \hat{\boldsymbol{w}}_{0:N-1}. \tag{19}$$

The subsequent result characterizes how the prediction error of $\hat{\boldsymbol{w}}_{0:N-1}$ influences control performance.

Define $V_0^{N,\mu}$ as the best achievable cost over horizon N, given that the first control action is fixed as $u_0 = \mu$

$$\begin{aligned} V_0^{N,\mu} :\ = \min_{u_1,\dots,u_{N-1}} & \sum_{k=0}^{N-1} L(x_k, u_k, w_k) + \tfrac{1}{2} x_N^\top P x_N \\ \text{s.t. } & x_{k+1} = Ax_k + B_u u_k + B_w w_k, \quad u_0 = \mu. \end{aligned}$$

Theorem 1: For an arbitrary bounded control law μ

$$V_0^{N,\mu} - V_0^{N^*} = \frac{1}{2} \left\| u_0^* - \mu \right\|^2_{R + B_u^\top P B_u}.$$

Proof: Observe that any bounded μ can be rewritten as $\mu = u_0^* + f_0$, where f_0 denotes the departure from the optimal control input u_0^*. The best achievable cost $V_0^{N,\mu}$, with the first control action fixed as μ, can be expressed in the following incremental form:

$$V_0^{N,\mu} = L(x_0, \mu, w_0) + V_1^{N-1^*} \tag{20}$$

where the second term $V_1^{N-1^*}$ depends on state x_1. By applying Lemma 2, using state x_1 and a prediction horizon of $N-1$, we get

$$V_1^{N-1^*} = \frac{1}{2} x_1^\top P x_1 + x_1^\top s_1 + a_1. \tag{21}$$

By substituting x_1, μ, and $V_1^{N-1^*}$ in (20) with $x_1 = Ax_0 + B_u\mu + B_w w_0$, $\mu = K_x x_0 + K_w w_0 + K_s s_1 + f_0$, and (21), respectively, (20) leads to

$$V_0^{N,\mu} = \frac{1}{2} x_0^\top P x_0 + x_0^\top s_0 + a_0 + \frac{1}{2} \|f_0\|^2_{R + B_u^\top P B_u} \tag{22}$$

where $a_0 = -1/2 \|K_w w_0 + K_s s_1\|^2_{R + B_u^\top P B_u} + 1/2 \|B_w w_0\|^2_P + w_0^\top B_w^\top s_1 + a_1$. Since $R + B_u^\top P B_u > 0$, V_0^N takes its minimum (optimal) value $V_0^{N^*}$ when $\mu = u_0^*$ and, for any bounded $\mu \neq u_0^*$, the associated cost satisfies

$$V_0^{N,\mu} = V_0^{N^*} + \frac{1}{2} \|f_0\|^2_{R + B_u^\top P B_u}$$

which completes the proof. □

Remark 3: With Theorem 1, the connection between the control problem of EM and the prediction problem of the WEF can be established by setting $\mu = \hat{u}_0^*$

$$\begin{aligned} V_0^{N,\hat{u}_0^*} - V_0^{N,*} &= \tfrac{1}{2} \left\| u_0^* - \hat{u}_0^* \right\|^2_{R + B_u^\top P B_u} \\ &= \tfrac{1}{2} \left\| K_d \left(\boldsymbol{w}_{0:N-1} - \hat{\boldsymbol{w}}_{0:N-1} \right) \right\|^2_{R + B_u^\top P B_u}. \end{aligned}$$

In Remark 3, $V_0^{N,\hat{u}_0^*} - V_0^{N^*}$ quantifies the performance loss incurred by using $\hat{u}_0^*$ instead of the optimal input u_0^*.

The estimation problem, with the consideration of control performance, is to parametrize an estimate of $\hat{\boldsymbol{w}}_{0:N-1}$, such that the expected cost for prediction

$$J_p := \mathbb{E} \left(\left\| K_d \left(\boldsymbol{w}_{0:N-1} - \hat{\boldsymbol{w}}_{0:N-1} \right) \right\|^2_{R + B_u^\top P B_u} \right) \tag{23}$$

is minimized. The factor $1/2$ is omitted for simplicity, as it does not affect the optimization outcome. In Section IV, a time-series-based predictor, that maximizes the energy output by minimizing the expected cost J_p, will be formulated.

IV. Predictions for LNOC

This section presents the predictor formulation. First, Section IV-A reviews the results of the WEF prediction using GP theory. Then, Section IV-B presents the formulation of the novel DE based on GPs, supported by theoretical statistical studies. Perfect knowledge of the wave spectrum will be assumed in Sections IV-A and IV-B to show the theoretical statistical properties. The implementation, including predictor formulation without using wave spectral information, will be discussed in Section IV-C.

A. GP-Based WEF Predictor

The result of a GP-based WEF predictor, developed and analyzed in [13], is initially recalled here.

Define the sequence of vectors of excitation force, $\boldsymbol{w}_{-H:-1}$ and $\boldsymbol{w}_{0:N-1}$ for the estimation problem as

$$X := [w_{H-1}, w_{H-2}, \dots, w_{-1}] \in \mathbb{R}^H \tag{24a}$$

$$Y := [w_0, w_1, \dots, w_N] \in \mathbb{R}^N. \tag{24b}$$

Following the properties of a linear stationary GP, the following variance-covariance matrices are determined by:

$$\Sigma_{XX} = \begin{bmatrix} r_0 & \dots & r_{H-1} \\ \vdots & \ddots & \vdots \\ r_{H-1} & \dots & r_0 \end{bmatrix}$$
$$\Sigma_{YY} = \begin{bmatrix} r_0 & \dots & r_{N-1} \\ \vdots & \ddots & \vdots \\ r_{N-1} & \dots & r_0 \end{bmatrix}$$
$$\Sigma_{XY} = \Sigma_{YX}^\top = \begin{bmatrix} r_H & \dots & r_{H+N-1} \\ \vdots & \ddots & \vdots \\ r_1 & \dots & r_N \end{bmatrix} \tag{25}$$

where each element r_i is the autocovariance function (ACVF) defined as

$$r_i := \mathbb{E}_k \left(w_k w_{k+i} \right). \tag{26}$$

Additionally, r_i takes its maximum value at $i = 0$, where $r_0 = \sigma^2$, where σ is the variance of the Gaussian process w_k.

Remark 4: The ACVF, defined in (26), can be obtained alongside the spectral density function (SDF) from the Fourier transform of w_k, according to the Wiener–Khintchine Theorem [13], [30].

To show the theoretical properties, in Sections IV-A and IV-B, the following assumptions are made.

Assumption 1: Suppose the following assumption holds for w_k.

1) Past information on the WEF, that is, w_k, $k \in \mathbb{Z}$, is perfectly known.
2) The WEF w_k can be modeled by a stationary, linear GP.
3) The ACVF of w_k, defined in (26), is available.

The optimal WEF prediction problem aims to minimize the expected accumulated prediction error

$$J_{\text{WEF}} = \mathbb{E}\left(\sum_{k=0}^{N-1} (w_k - \hat{w}_k) \right) \tag{27}$$

for a direct multistep (DMS) WEF predictor structure

$$\hat{\boldsymbol{w}}_{0:N-1} = \Theta_{\text{GP-WEF}} \boldsymbol{w}_{-H:-1} \tag{28}$$

where $\Theta_{\text{GP-WEF}} \in \mathbb{R}^{N \times H}$ is the predictor coefficient to be determined.

Next, WEF predictor is parameterized using GP theory. When X is known, the conditional distribution of Y, given X, $Y|X$, is also described by a multivariate Gaussian distribution [31], with a conditional mean $\mu_{Y|X}$ and a variance $\Sigma_{Y|X}$

$$\begin{aligned} \mu_{Y|X} &= \Sigma_{YX} \Sigma_{XX}^{-1} X \\ \Sigma_{Y|X} &= \Sigma_{YY} - \Sigma_{YX} \Sigma_{XX}^{-1} \Sigma_{XY}. \end{aligned} \tag{29}$$

Therefore, the prediction of $\boldsymbol{w}_{0:N-1}$ is given by $\mu_{Y|X}$ as

$$\hat{\boldsymbol{w}}_{0:N-1} = \mu_{Y|X} = \Theta_{\text{GP-WEF}} \boldsymbol{w}_{-H:-1} \tag{30}$$

with the optimal estimator coefficient

$$\Theta_{\text{GP-WEF}} := \Sigma_{YX} \Sigma_{XX}^{-1}. \tag{31}$$

The predictor in (30) is termed the "theoretically optimal predictor" in [13], which, under the assumption of a perfectly known ACVF, minimizes the accumulated WEF prediction error (27). However, as shown in Section III, to optimize EM control performance, the WEF predictor must be evaluated by the cost function for prediction J_p, defined in (23).

As $X := \boldsymbol{w}_{-H:-1}$ has already occurred, the conditional covariance given X coincides with the covariance. Therefore, the corresponding cost function for prediction (23), when the GP-based optimal WEF predictor (30) is used, can be calculated as

$$\begin{aligned} J_{\text{GP-WEF}} &:= \mathbb{E}\left(\| K_d (\boldsymbol{w}_{0:N-1} - \hat{\boldsymbol{w}}_{0:N-1}) \|^2_{R + B_u^\top P B_u} \right) \\ &= \mathbb{E}\left(\| K_d (\boldsymbol{w}_{0:N-1} - \hat{\boldsymbol{w}}_{0:N-1}) \|^2_{R + B_u^\top P B_u} \, | X \right) \\ &= K_d \, \mathbb{E}\left(\| (\boldsymbol{w}_{0:N-1} - \hat{\boldsymbol{w}}_{0:N-1}) \|^2 \, | X \right) K_d^\top \left(R + B_u^\top P B_u \right) \\ &= K_d \left(\Sigma_{YY} - \Sigma_{YX} \Sigma_{XX}^{-1} \Sigma_{XY} \right) K_d^\top \left(R + B_u^\top P B_u \right). \end{aligned} \tag{32}$$

B. DE Formulation for the Acausal Part

Since, to optimize control performance, the goal of excitation force prediction is to minimize the deviation between $\hat{u}_{ff,0} = K_d \hat{\boldsymbol{w}}_{0:N-1}$ and $u_{ff,0} = K_d \boldsymbol{w}_{0:N-1}$, the linear GP model can be modified to directly construct $\hat{u}_{ff,0}$.

Recall X and Y defined in (24). To formulate the GP-based DE, a new parameter to be estimated is introduced as

$$Z := u_{ff,0} = K_d Y \in \mathbb{R}. \tag{33}$$

The corresponding variance/covariance matrices of the augmented vector $[X, Z]$, that is, Σ_{XX}, Σ_{XZ}, Σ_{ZX}, and Σ_{ZZ}, satisfy

$$\begin{bmatrix} \Sigma_{XX} & \Sigma_{XZ} \\ \Sigma_{ZX} & \Sigma_{ZZ} \end{bmatrix} = \begin{bmatrix} I & \\ & K_d \end{bmatrix} \begin{bmatrix} \Sigma_{XX} & \Sigma_{XY} \\ \Sigma_{YX} & \Sigma_{YY} \end{bmatrix} \begin{bmatrix} I & \\ & K_d^\top \end{bmatrix}$$

which leads to

$$\Sigma_{XZ} = \Sigma_{ZX}^\top = \Sigma_{XY} K_d^\top, \quad \Sigma_{ZZ} = K_d \Sigma_{YY} K_d^\top. \tag{34}$$

Similarly, with known X, the conditional distribution of Z, given X, $Z|X$, is also described by a multivariate Gaussian distribution [31], and the conditional mean $\mu_{Z|X}$ and variance $\Sigma_{Z|X}$ satisfy

$$\begin{aligned} \mu_{Z|X} &= \Sigma_{ZX} \Sigma_{XX}^{-1} X, \\ \Sigma_{Z|X} &= \Sigma_{ZZ} - \Sigma_{ZX} \Sigma_{XX}^{-1} \Sigma_{XZ}. \end{aligned}$$

Therefore, the direct estimate of $u_{ff,0}$ is given by

$$\hat{u}_{ff,0} = \mu_{Z|X} = \Theta_{\text{GP-DE}} \boldsymbol{w}_{-H:-1} = \Sigma_{ZX} \Sigma_{XX}^{-1} \boldsymbol{w}_{-H:-1} \tag{35}$$

where the optimal parameters of the DE

$$\Theta_{\text{GP-DE}} := \Sigma_{ZX} \Sigma_{XX}^{-1} \in \mathbb{R}^{1 \times H} \tag{36}$$

only require H parameters to be determined.

With the DE formulated in (35), the corresponding cost function for this direct u_{ff} estimator $J_{\text{GP-DE}}$, defined in (23), when using the estimator (35), takes the value of

$$\begin{aligned} J_{\text{GP-DE}} &:= \mathbb{E}\left(\| K_d (\boldsymbol{w}_{0:N-1} - \hat{\boldsymbol{w}}_{0:N-1}) \|^2_{R + B_u^\top P B_u} \right) \\ &= \mathbb{E}\left(\left\| \hat{u}_{ff,0} - u_{ff,0} \right\|^2_{R + B_u^\top P B_u} \right) \\ &= \mathbb{E}\left(\left\| \hat{u}_{ff,0} - u_{ff,0} \right\|^2 | X \right) \left(R + B_u^\top P B_u \right) \\ &= \left(\Sigma_{ZZ} - \Sigma_{ZX} \Sigma_{XX}^{-1} \Sigma_{XZ} \right) \left(R + B_u^\top P B_u \right). \end{aligned} \tag{37}$$

The statistical relations between the GP-based WEF predictor (30) and the GP-based DE (35) are established in the following Theorem.

Theorem 2: Suppose Assumption 1 holds. The calculation of u_0^* using the GP-based WEF predictor (30)

$$\hat{u}_0^* = K_x x_0 + K_d \Theta_{\text{GP-WEF}} \boldsymbol{w}_{-H:-1}$$

and using the GP-based DE (35)

$$\hat{u}_0^* = K_x x_0 + \Theta_{\text{GP-DE}} \boldsymbol{w}_{-H:-1}$$

lead to an identical result for all bounded sequences $\boldsymbol{w}_{-H:-1} \in \mathbb{R}^H$. Moreover, both methods of constructing $\hat{u}_0^*$ lead to optimal control performance, in the sense that fully accurate information on the future WEF is unavailable and a linear AR predictor is used.

Remark 5: Theorem 2 shows that the novel GP-based DE achieves the same statistical optimal performance as the GP-based WEF predictor, but has significantly fewer determining parameters (H parameters for DE compared with $N \times H$ parameters for the WEF predictor), making it easier to formulate without spectrum information, and easier to adapt to the change of sea states.

Proof: The equivalence of cost can be established by comparing $J_{\text{GP-WEF}}$ and $J_{\text{GP-DE}}$ in (32) and (37), respectively, and using the relation in (34).

To show optimality, one first observes from (37) that, since $R + B_u^\top P B_u$ is a fixed scalar, minimizing J_p is equivalent to minimizing

$$\mathbb{E}\left(\left\| \hat{u}_{ff,0} - u_{ff,0} \right\|^2 | X \right)$$

which can be solved by the GP-based DE (36) [31]. This implies that the GP-based DE solves the optimal estimation problem (23). Therefore, the proof is completed by applying Theorem 1 to establish the connection between the optimal control problem and the optimal estimation problem. □

So far, the GP-based DE has been formulated and its theoretical statistical properties studied based on the idealized, but unrealistic, Assumption 1. In Section IV-C, the implementation challenges for nonideal cases will be addressed.

C. Implementation

When WEF spectral information is unavailable, or the sea state changes gradually, a practical approach is to identify Θ_{DE} using operational data. By converting the stored data into $(\boldsymbol{w}_{k-H:k-1}, u_{ff,k} = K_d \boldsymbol{w}_{k:k+N-1})$ for $k \in \mathbb{Z}_{1:N_r}$, with N_r denoting the number of the data points collected, the parameterization problem for Θ_{DE} can be written as

$$\hat{\Theta}_{\text{DE}}^* = \arg\min_{\Theta_{\text{DE}}} \sum_{k=1}^{N_r} \left\| \Theta_{\text{DE}} \boldsymbol{w}_{k-H:k-1} - u_{ff,k} \right\|^2_{R + B_u^\top P B_u} \tag{38}$$

using linear least squares (LLS) methods. For completeness, the following training using batch least squares (BLS) is employed for demonstration, though other LLS methods like recursive least squares (RLS) can also be used:

$$\hat{\Theta}_{\text{DE}}^* = \left[\left(X_{\text{BLS}}^\top W X_{\text{BLS}} \right)^{-1} X_{\text{BLS}}^\top W Y_{\text{BLS}} \right]^\top \tag{39}$$

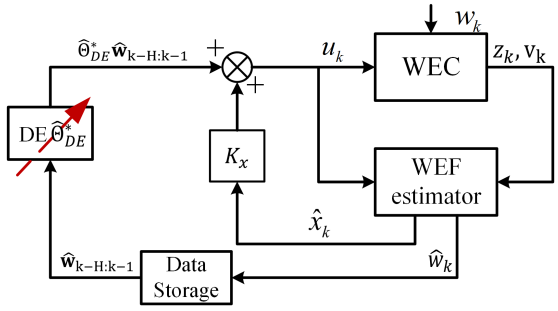

Fig. 2. Causal framework to implement LNOC, consisting of (a) control law $u_k = K_x \hat{x}_k + \hat{\Theta}^*_{\text{DE}} \hat{\boldsymbol{w}}_{k-H:k-1}$, (b) WEF estimator, and (c) DE $\hat{\Theta}^*_{\text{DE}}$ for $u_{ff,k}$ estimation.

where $X_{\text{BLS}} := [\boldsymbol{w}_{1-H:0}, \ \boldsymbol{w}_{2-H:1} \ \ldots \ \boldsymbol{w}_{N_r-H:N_r-1}]^\top$, $Y_{\text{BLS}} := [K_d \boldsymbol{w}_{1:N} \ K_d \boldsymbol{w}_{2:N+1} \ \ldots \ K_d \boldsymbol{w}_{N_r:N_r+N-1}]^\top$, and $W := R + B_u^\top P B_u$.

For most WECs, due to the nonmeasurable nature of WEF and radiation force states, observers are needed to estimate x and w.

The WEF estimator design problem, focused on estimating x_k under unknown disturbance w_k, is a well-studied problem (see [32] for a benchmark study on several popular WEF estimators). As detailed WEF estimation is beyond the scope of this brief, interested readers are referred to [32] for the design details.

With the WEF estimator from [32], and the proposed DE for the acausal part, the noncausal control framework can be realized using a simple-to-implement causal block diagram, as shown in Fig. 2.

V. Numerical Simulation

In this section, numerical simulations are presented, based on a benchmarked PA type WEC with the parameters adopted from [10] and [33]. The state-space approximation of the radiation dynamics (3) is

$$A_r = \begin{bmatrix} 0 & 0 & -17.9 \\ 1 & 0 & -17.7 \\ 0 & 1 & -4.41 \end{bmatrix}, \quad B_r = \begin{bmatrix} 38.6 \\ 379 \\ 89 \end{bmatrix}$$
$$C_r = \begin{bmatrix} 0 \\ 0 \\ 1 \end{bmatrix}^\top, \quad D_r = 0.$$

The simulation parameters are $r = 5 \times 10^{-3}$ for (8), and sampling period $t_s = 0.1$ s. Based on [32, Sec. II-D], a WEF estimator is designed to reconstruct full state information x at the current time step k and the WEF w up to time step $k-1$.

After solving DARE (14) for P, the control coefficient $K_x = \begin{bmatrix} 32.59 & -54.31 & 0.75 & -1.95 & -5.40 \end{bmatrix}$ is calculated from (15), and K_d from (17), shown in Fig. 3.

The DE is formulated based on the available wave spectral information. The simulation uses a segment of the WEF, shown in Fig. 4(a), generated from a JONSWAP spectrum, with a significant wave height $H_s = 2.5$ m, peak period $T_p = 4$ s, and peakedness factor $\lambda = 3.3$.[1]

[1]A slight shift in T_p is introduced to avoid the repetitive nature of the JONSWAP wave, starting from $T_p = 4$ s at the beginning of the simulation and increasing to $T_p = 4.005$ s by the end of the 200-s simulation.

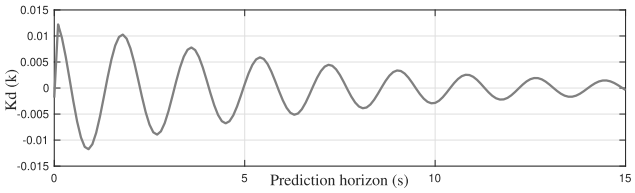

Fig. 3. Feedforward coefficient K_d, whose magnitude converges to zero as the prediction step increases, due to the asymptotic stability of the closed-loop system $\Phi := (A + B_u K_x)^\top$.

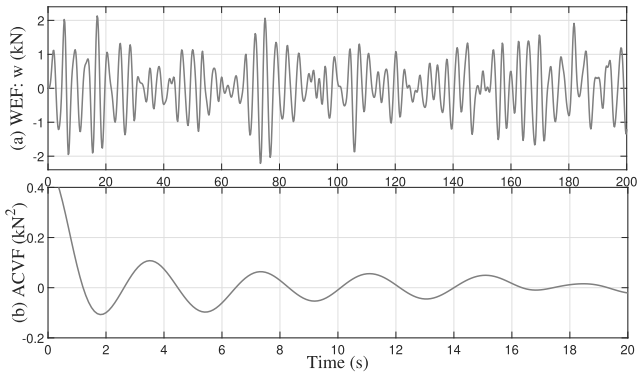

Fig. 4. (a) 200-s WEF used for simulation, generated from a JONSWAP spectrum, with a significant wave height $H_s = 2.5$ m, peak period $T_s = 4.5$ s, and peakedness factor $\lambda = 3.3$. (b) ACVF, calculated from the inverse Fourier transform of the available WEF SDF.

The ACVF r_i is calculated by applying an inverse Fourier transform to the available SDF, with the ACVF profile shown in Fig. 4(b). Then, the parameter of the DE $\Theta_{\text{GP-DE}}$ is calculated from (36), where Σ_{XX} and Σ_{XY} are determined from the ACVF by (25), and Σ_{ZZ} is calculated from (34), respectively.

Next, a time simulation is presented, based on the WEF profile shown in Fig. 4(a), using the following controllers.

1) *"Causal:"* $u_k = K_x x_k$, using no WEF prediction.
2) *"Accurate:"* $u_k = K_x x_k + K_d \boldsymbol{w}_{k:k+N-1}$, using 100% accurate WEF prediction.
3) *"GP-WEF:"* $u_k = K_x x_k + K_d \Theta_{\text{GP-WEF}} \boldsymbol{w}_{k-H:k-1}$, using the GP-based WEF predictor parameterized with (31).
4) *"GP-DE:"* $u_k = K_x x_k + \Theta_{\text{GP-DE}} \boldsymbol{w}_{k-H:k-1}$, using the novel DE parameterized with (36).
5) *"LLS-DE:"* $u_k = K_x x_k + \hat{\Theta}^*_{\text{DE}} \boldsymbol{w}_{k-H:k-1}$, using the novel DE parameterized using LLS (39), based on 2 min of collected data.

Fig. 5(a) shows a 200 s simulation, with a WEF prediction horizon of 8 s (corresponding to 2× the peak period), and a look-back horizon of 30 steps (corresponding to 3 s). As in the formulation process, $K_d \Theta_{\text{GP-WEF}} = \Theta_{\text{GP-DE}}$, GP-WEF and GP-DE lead to identical results, with 5.24 kJ generated, compared with 5.54 kJ generated with LNOC with accurate WEF prediction, and 5.22 kJ using LLS-DE parameterized from 2 min of training data. All three LNOC with realistic predictors significantly outperform the causal controller of 4.67 kJ, by at least 11.78%.

To further test the efficacy of DE, the WEF prediction horizon is varied from 0.1 to 15 s. As shown in Fig. 5(b), LNOC with the ideal, but unrealistic, accurate WEF

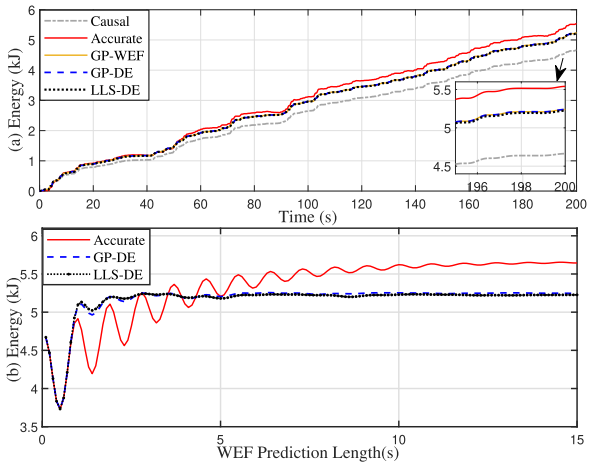

Fig. 5. Simulation results based on WEF profile shown in Fig. 4(a). (a) Accumulated energy produced by all five controllers (time simulation) with a WEF prediction length of 8 s. (b) Accumulated energy produced versus different WEF prediction lengths N (comparison across prediction scenarios).

prediction generates more energy as the prediction horizon increases. Meanwhile, the DE, with both parameterization methods, demonstrates similar performance. Specifically, the DE, parameterized using only 120 s of data collected during operation, achieves over 99.5% of the performance of the DE, parameterized using a GP and the available WEF spectrum information. This highlights a major advantage of the LLS-DE approach, since it adapts more quickly to changing sea states. This benefit arises from the novel DE formulation, which significantly reduces the number of parameters to be determined.

VI. Conclusion

This brief examines the WEF prediction problem in the context of LNOC for WECs with linear dynamics. By investigating the relationship between the optimal control problem and the optimal WEF prediction problem, a novel DE is developed to estimate the acausal component of the LNOC. This new approach is both optimal and simple to parametrize. Numerical simulation demonstrates the effectiveness of the proposed methods, paving the way for the development of a near-optimal causal control framework, having the wave predictor integrated, with enhanced theoretical guarantees. These findings offer significant potential for improving the practical implementation of WEC control systems. It is worth noting that, in this work, input and state constraints were not considered in order to derive a closed-form analytic solution of LNOC. In future work, we will extend the results to a model-predictive control framework for WEC EM, where safety constraints on states and inputs, as well as nonlinearities, can be incorporated.

References

[1] *Innovation Outlook: Ocean Energy Technologies*, International Renewable Energy Agency (IRENA), 2020. [Online]. Available: https://www.irena.org/Publications/2020/Dec/Innovation-Outlook-Ocean-Energy-Technologies

[2] J. V. Ringwood, G. Bacelli, and F. Fusco, "Energy-maximizing control of wave-energy converters: The development of control system technology to optimize their operation," *IEEE Control Syst. Mag.*, vol. 34, no. 5, pp. 30–55, Oct. 2014.

[3] J. V. Ringwood, S. Zhan, and N. Faedo, "Empowering wave energy with control technology: Possibilities and pitfalls," *Annu. Rev. Control*, vol. 55, pp. 18–44, 2023.

[4] N. Faedo, S. Olaya, and J. V. Ringwood, "Optimal control, MPC and MPC-like algorithms for wave energy systems: An overview," *IFAC J. Syst. Control*, vol. 1, pp. 37–56, Sep. 2017.

[5] G. Li, G. Weiss, M. Mueller, S. Townley, and M. R. Belmont, "Wave energy converter control by wave prediction and dynamic programming," *Renew. Energy*, vol. 48, pp. 392–403, Dec. 2012.

[6] S. Zhan, J. Na, and G. Li, "Nonlinear noncausal optimal control of wave energy converters via approximate dynamic programming," *IEEE Trans. Ind. Informat.*, vol. 15, no. 11, pp. 6070–6079, Nov. 2019.

[7] G. Li and M. R. Belmont, "Model predictive control of sea wave energy converters—Part I: A convex approach for the case of a single device," *Renew. Energy*, vol. 69, pp. 453–463, Sep. 2014.

[8] A. Karthikeyan, M. Previsic, J. T. Scruggs, and A. Chertok, "Non-linear model predictive control of wave energy converters with realistic power take-off configurations and loss model," in *Proc. IEEE Conf. Control Technol. Appl. (CCTA)*, Aug. 2019, pp. 270–277. [Online]. Available: https://ccta2019.ieeecss.org/registration/

[9] A. S. Haider, T. K. A. Brekken, and A. McCall, "Application of real-time nonlinear model predictive control for wave energy conversion," *IET Renew. Power Gener.*, vol. 15, no. 14, pp. 3331–3340, Oct. 2021.

[10] S. Zhan and G. Li, "Linear optimal noncausal control of wave energy converters," *IEEE Trans. Control Syst. Technol.*, vol. 27, no. 4, pp. 1526–1536, Jul. 2019.

[11] S. Zhan and J. V. Ringwood, "Model-free linear noncausal optimal control of wave energy converters via reinforcement learning," *IEEE Trans. Control Syst. Technol.*, vol. 32, no. 6, pp. 2164–2177, Nov. 2024.

[12] P. K. Stansby and E. C. Moreno, "Hydrodynamics of the multi-float wave energy converter M4 with slack moorings: Time domain linear diffraction-radiation modelling with mean force and experimental comparison," *Appl. Ocean Res.*, vol. 97, Apr. 2020, Art. no. 102070.

[13] Y. Peña-Sanchez, A. Mérigaud, and J. V. Ringwood, "Short-term forecasting of sea surface elevation for wave energy applications: The autoregressive model revisited," *IEEE J. Ocean. Eng.*, vol. 45, no. 2, pp. 462–471, Apr. 2020.

[14] M. P. Schoen, J. Hals, and T. Moan, "Wave prediction and robust control of heaving wave energy devices for irregular waves," *IEEE Trans. Energy Convers.*, vol. 26, no. 2, pp. 627–638, Jun. 2011.

[15] F. Fusco and J. V. Ringwood, "A study of the prediction requirements in real-time control of wave energy converters," *IEEE Trans. Sustain. Energy*, vol. 3, no. 1, pp. 176–184, Jan. 2012.

[16] Z. Liao, N. Gai, P. Stansby, and G. Li, "Linear non-causal optimal control of an attenuator type wave energy converter M4," *IEEE Trans. Sustain. Energy*, vol. 11, no. 3, pp. 1278–1286, Jul. 2020.

[17] M. Penalba, G. Giorgi, and J. V. Ringwood, "Mathematical modelling of wave energy converters: A review of nonlinear approaches," *Renew. Sustain. Energy Rev.*, vol. 78, pp. 1188–1207, Oct. 2017.

[18] F. Fusco and J. V. Ringwood, "Short-term wave forecasting for real-time control of wave energy converters," *IEEE Trans. Sustain. Energy*, vol. 1, no. 2, pp. 99–106, Jul. 2010.

[19] A. Mérigaud and J. V. Ringwood, "Incorporating ocean wave spectrum information in short-term free-surface elevation forecasting," *IEEE J. Ocean. Eng.*, vol. 44, no. 2, pp. 401–414, Apr. 2019.

[20] A. Babarit and G. Delhommeau, "Theoretical and numerical aspects of the open source BEM solver NEMOH," in *Proc. 11th Eur. Wave Tidal Energy Conf. (EWTEC)*, Nantes, France, Sep. 2015, pp. 1–12.

[21] W. E. Cummins, "The impulse response function and ship motions," *Schiffstechnik*, vol. 47, no. 9, pp. 101–109, 1962. [Online]. Available: https://ee.maynoothuniversity.ie/jringwood/Respubs/J541OEChenZhan.pdf

[22] Y. Lao, J. T. Scruggs, A. Karthikeyan, and M. Previsic, "Discrete-time causal control of a wave energy converter with finite stroke in stochastic waves," *IEEE Trans. Control Syst. Technol.*, vol. 30, no. 3, pp. 1198–1214, May 2022.

[23] N. Faedo, Y. Peñ-Sanchez, F. Carapellese, G. Mattiazzo, and J. V. Ringwood, "LMI-based passivation of LTI systems with application to marine structures," *IET Renew. Power Gener.*, vol. 15, no. 14, pp. 3424–3433, Oct. 2021.

[24] N. Faedo, Y. Peña-Sanchez, and J. V. Ringwood, "Passivity preserving moment-based finite-order hydrodynamic model identification for wave energy applications," *Adv. Renew. Energies Offshore*, pp. 351–359, Nov. 2018.

[25] A. Kody, N. Tom, and J. T. Scruggs, "Model predictive control of a wave energy converter using duality techniques," in *Proc. Amer. Control Conf. (ACC)*, 2019, pp. 5444–5451.

[26] S. Zhan, Y. Chen, and J. V. Ringwood, "Terminal weight and constraint design for wave energy converter economic model predictive control problems," *Int. J. Robust Nonlinear Control*, vol. 35, no. 7, pp. 2694–2716, May 2025.

[27] O. I. Olanrewaju and J. M. Maciejowski, "Implications of dissipativity on stability of economic model predictive control—The indefinite linear quadratic case," *Syst. Control Lett.*, vol. 100, pp. 43–50, Feb. 2017.

[28] M. Zanon, S. Gros, and M. Diehl, "Indefinite linear MPC and approximated economic MPC for nonlinear systems," *J. Process Control*, vol. 24, no. 8, pp. 1273–1281, Aug. 2014.

[29] S. Zhan, P. Stansby, Z. Liao, and G. Li, "A fast model predictive control framework for multi-float and multi-mode-motion wave energy converters," *IEEE Trans. Control Syst. Technol.*, vol. 31, no. 3, pp. 1443–1450, May 2023.

[30] A. Mérigaud and J. V. Ringwood, "Free-surface time-series generation for wave energy applications," *IEEE J. Ocean. Eng.*, vol. 43, no. 1, pp. 19–35, Jan. 2018.

[31] C. E. Rasmussen and C. K. Williams, *Gaussian Processes for Machine Learning*, vol. 1. Cham, Switzerland: Springer, 2006.

[32] Y. Peña-Sanchez, C. Windt, J. Davidson, and J. V. Ringwood, "A critical comparison of excitation force estimators for wave-energy devices," *IEEE Trans. Control Syst. Technol.*, vol. 28, no. 6, pp. 2263–2275, Nov. 2020.

[33] Z. Yu and J. Falnes, "State-space modelling of a vertical cylinder in heave," *Appl. Ocean Res.*, vol. 17, no. 5, pp. 265–275, Oct. 1995.